

Nucleation of Bulk Phases in the HCl/H₂O System

Bryan F. Henson,* Kevin R. Wilson,† Jeanne M. Robinson, Christopher A. Nobel,‡
Joanna L. Casson, Laura F. Voss,§ and Douglas R. Worsnop||

Los Alamos National Laboratory, Los Alamos, New Mexico 87545

Received: June 4, 2007

We report experimental results on the low-temperature uptake of HCl on H₂O ice (ice). HCl was deposited on the surface at greater than monolayer amounts at 85 K, and the ice substrate was heated. The temperature dependence of the HCl vapor pressure from this phase was measured from 110 to 150 K, with the nucleation of a bulk hydrate phase observed at 150 K. Measurements were conducted in a closed system by simultaneous application of gas phase mass spectrometry and surface spectroscopy to characterize vapor/solid equilibrium and the nucleation of bulk hydrate phases. Combining the nucleation data reported here with data we reported previously (180 to 200 K) and data from two other laboratories (165 and 170 K), the thermodynamic boundaries for the nucleation of both the metastable bulk solution and bulk hydrate phases subsequent to monolayer adsorption of HCl have been determined. The nucleation of the metastable bulk solution phase occurs promptly at monolayer coverage at the ice/liquid coexistence boundary on the binary bulk phase diagram. The nucleation of the bulk hexahydrate occurs from this metastable solution along a locus of points defining a state of constant solution free energy. This measured free energy is -51.2 ± 0.9 kJ/mol. Finally, the temperature dependence of the HCl vapor pressure from the low-temperature phase is reported here for the first time and is consistent with that of the metastable solution predicted by this thermodynamic model of uptake, extending the range of validity of this model of adsorption followed by bulk solution and hydrate nucleation to a lower bound in temperature of 110 K.

Introduction

The physical state of HCl adsorbed on ice is of interest given the effect of acidity on chemical reactions in the adsorbed phase. It is also of specific importance with respect to the role of heterogeneous chlorine activation in the upper atmosphere.¹ In an earlier publication,² submonolayer adsorption of HCl on H₂O ice at temperatures between 180 K and the hexahydrate melting point (~ 202 K) was found to be well described by a model of single-layer adsorption that includes the complete dissociation of HCl into H⁺ and Cl⁻ ions. Adsorption is consistent with two distinct states on the ice substrate, one in which the ions each adsorb to a separate site with very low adsorption energy and another where the ions adsorb as an H⁺-Cl⁻ pair on a single site with adsorption energy similar to the bulk phases of the HCl/H₂O system at these temperatures. The relative surface concentration of these states is controlled by a temperature-dependent equilibrium constant. The measured area per site exhibited by this phase, equivalent to ~ 5 surface H₂O molecules, is consistent with the stoichiometry of these bulk phases. This model of adsorption provides a detailed picture of the adsorption of HCl on ice which is consistent with the bulk thermodynamics of this binary system.

An important component of that work² was also the observation of nucleation boundaries, where the system undergoes a transition to true bulk behavior that is no longer governed by adsorption. These boundaries are very important from the point of view of experiments designed to simulate specific environ-

mental conditions, particularly the conditions of the upper troposphere and lower stratosphere. In this work we present additional measurements of HCl partial pressure in this system at temperatures lower than previously reported, from 110 to 150 K, that further define the boundaries of nucleation of both metastable and equilibrium bulk phases. We also present nonlinear light scattering results utilizing second harmonic generation (SHG) which suggest that 110 K represents the lower bound in temperature of the applicability of this model of HCl adsorption/nucleation.

These measurements also enhance our understanding of the state of dissociation of HCl on the ice surface. There has been considerable discussion in the literature regarding the state of HCl adsorbed onto the H₂O ice surface at low temperatures.³ Low-temperature spectroscopic studies of adsorption on nanocrystalline ice surfaces have indicated molecular HCl at temperatures as high as 125 K,⁴ and the appearance of ionic-like dissociative adsorption from 60 to 90 K.³ Other spectroscopic studies indicate complete ionization at higher temperatures.^{5,6} In a measurement of the dissociative electron cross-section of HCl on ice, Sanche et al. observed dissociation at low temperature.⁷ In other experiments above ~ 100 K, a temperature-dependent state of ionization was reported using Cs⁺ ion scattering,^{8,9} and complete dissociation was measured by secondary ion mass spectrometry (SIMS)¹⁰ and near edge X-ray fine structure (NEXAFS).¹¹ Electron impact ionization results indicate a dissociated state of HCl adsorbed on crystalline ice at 140 K.¹² The measurements presented here indicate a bulk state of dissociation (metastable solution) to temperatures as low as 110 K.

Finally, although we present these results as confirming and extending the validity of our model of adsorption and nucleation

* Corresponding author. E-mail: henson@lanl.gov.

† Lawrence Berkeley National Laboratory, Berkeley, CA 94720.

‡ Northrop Grumman, Fairfax, VA 22033.

§ Department of Chemistry, Bowdoin College, Brunswick, ME 04011.

|| Aerodyne Research, Inc., Billerica, MA 01821.

in the HCl/ice system, it is explicitly a model of metastable phase formation and a specific pathway to the stable equilibrium phases of the system. It is also a model of the HCl/ice system valid in the range of HCl activity (concentration) corresponding to monolayer coverage of HCl on ice and the resulting equilibrium vapor pressure. Other pathways toward stable hydrate formation are possible, including the hexahydrate discussed here, if higher levels of HCl chemical activity are applied to the binary system. A specific example is the considerable work performed on measuring the kinetics of hydrate formation subsequent to nucleation at low temperatures.^{13,14}

Experimental Details

The experiments were conducted as described in ref 2. A measured flow of HCl vapor was introduced into a closed system containing a temperature-controlled ice sample of known total surface area. Ice samples (0.5 g) were prepared by vapor deposition over 1 h onto a 50 cm² brass support at 85 K. Heating the samples under vacuum to temperatures between 190 and 260 K resulted in controllable ice surface area density from 8 to 100 m²/g. The area density of the ice samples was measured by argon physical adsorption with standard Brunauer–Emmett–Teller (BET) analysis.¹⁵ Repeated measurement of the surface area resulting from a given annealing profile demonstrated a standard deviation of 20% in the surface area. In addition, this annealing insured that all low-temperature glass or amorphous phases were fully converted to hexagonal ice I_h before the low-temperature introduction of HCl. This ice characterization was made in situ, and the measured properties are thus identical, within 20%, to those for ice samples used in the HCl adsorption experiments. Substrate temperature was monitored via thermocouples soldered directly to the brass support. Temperature control in these experiments was obtained by flowing N₂ gas through the support in concert with a resistive heater mounted within the support. Excellent agreement was obtained between measured H₂O vapor pressure from the pure ice as a function of temperature with accepted values.¹⁶ Partial vapor pressures were measured with a quadrupole mass spectrometer. The pressure calibration for H₂O vapor was made by direct comparison of mass spectrometer signals to pressure transducers in the 10⁻³ Torr range. The pressure calibration for HCl was then made by direct comparison to H₂O signals and utilizing a constant factor to correct for ionization potentials.

The amount of HCl deposited on the ice was calculated from the measured HCl flow into the chamber. This assumes that all HCl condenses on the ice surface, an excellent approximation in this apparatus.² The sensitivity in these measurements was determined to be $\sim 3 \times 10^{-7}$ Torr for HCl, with an absolute accuracy of 30%. An independent confirmation of these calibrations is provided by comparison of measured partial vapor pressures to the bulk phase diagram of HCl/H₂O in the hydrate and liquid regimes subsequent to nucleation of the samples in some experiments, as was demonstrated in ref 2. The stability of the mass spectrometer (MS) signals with time was rigorously demonstrated in ref 2. The MS signals for HCl or H₂O did not vary by more than 30% subsequent to halting the introduction of HCl. This was tested on many occasions at different temperatures along the HCl isotherm and over times from minutes to an hour.² These stability tests were performed to ensure accurate vapor pressure measurements, unperturbed by the time constant for permeation into the ice, wall loss, and loss to the mass spectrometer itself.

To obtain the SHG signal, the ice films were illuminated by weakly focused 532 nm light from a Nd:YAG laser, operated

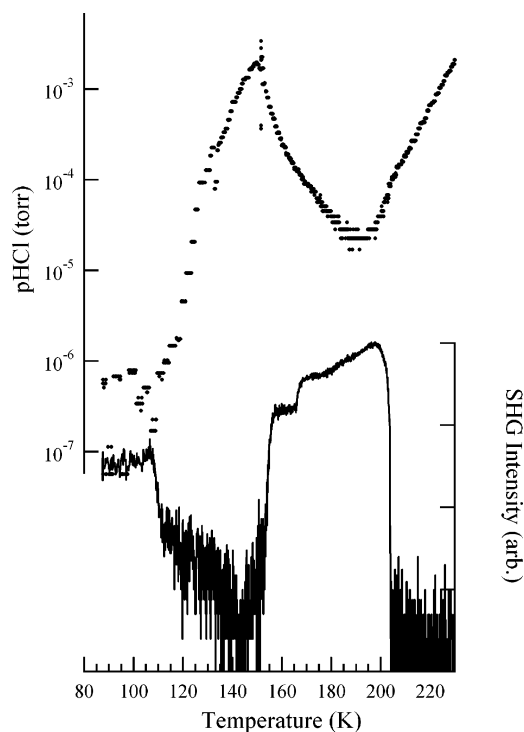


Figure 1. Heating of an HCl phase on ice adsorbed at low temperature. Initially 7.92×10^{-4} mol were deposited on an 80 m² ice at 85 K. The sample was then heated at 0.05 K/s. The HCl vapor pressure (pHCl) is plotted as the points, and the observed SHG intensity is plotted on a logarithmic scale as the black line. Both are plotted as a function of the ice sample temperature.

at 10 Hz with ~ 35 ps pulsewidth and 100 μ J energy per pulse. The second harmonic light was directed to a monochromator centered at 266 nm and detected by a gated photomultiplier tube.

Results

A. Low-Temperature Adsorption and Heating. The first experiments involved low-temperature adsorption of an amount of HCl with subsequent heating. At the low temperatures during adsorption, the HCl and ice vapor pressures (pHCl and pH₂O) were below detection limits. During subsequent heating, pHCl was eventually detectable and the dependence of pHCl on temperature was measured. The observed SHG intensity from the surface was used, as in ref 2, to monitor the melting and nucleation of bulk phases. Experiments using this temperature and concentration profile were conducted several times with reproducible results. The results of one such experiment are shown in Figure 1. Initially 7.92×10^{-4} mol of HCl were deposited onto an 80 m² ice sample at 85 ± 2 K. This amount of HCl is assumed constant throughout the experiment, an approximation better than 10^{-4} under these conditions in this apparatus due to the ice surface area to chamber volume ratio.² The HCl vapor pressure was below the 3×10^{-7} Torr minimum sensitivity throughout adsorption. The substrate was then heated at approximately 0.05 K/s. In Figure 1, pHCl is plotted as points in the top panel. pHCl was observed to rise above detection sensitivity at 110 K and eventually reached very high levels. Co-incident with this rise in pHCl is a drop in the SHG intensity, plotted at the bottom panel of the figure as the black line. The SHG intensity decreased from the signal observed from pure ice to a level below detection sensitivity at 110 K. An abrupt drop in pHCl was then observed at approximately 152 K, and this drop in pHCl just preceded an observed increase in the SHG intensity at 156 K. The SHG intensity was observed to

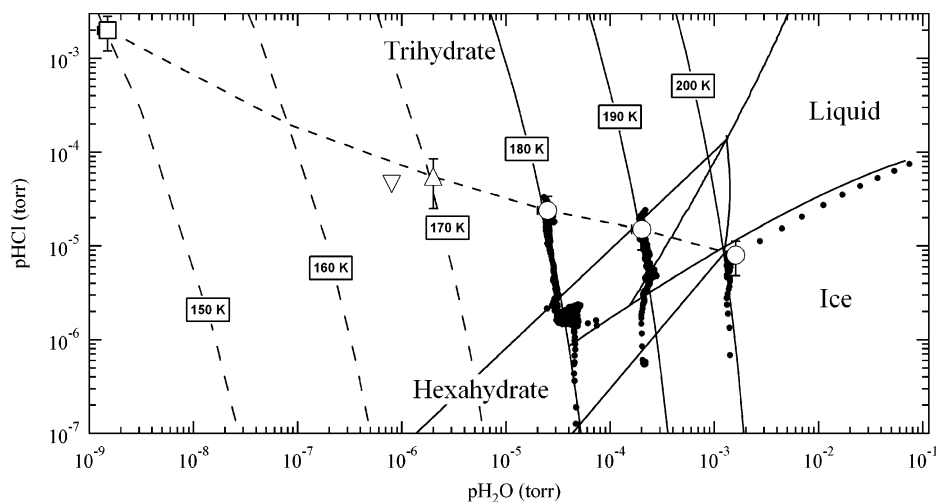


Figure 2. Adsorption and nucleation data superimposed on the HCl/H₂O bulk phase diagram. The data points are from adsorption experiments where HCl is introduced over ice. The open points mark observations of nucleation of the hexahydrate in this and other laboratories, discussed in the text. The triangle data point is plotted with vertical bars, and the circles and squares contain vertical and horizontal bars. The black dashed line denotes the locus of points defining the hexahydrate nucleation boundary as a state of constant solution free energy, also discussed in the text.

evolve during continued warming of the ice while pHCl decreased steadily. Although some structure is apparent in the SHG intensity from 156 to 202 K, the observation pertinent to the results here is that significant intensity appears at 156 K, persists at some nearly constant level, and disappears abruptly at 202 K. At 202 K, co-incident with the loss of SHG intensity, pHCl again increases and increases steadily until the end of the experiment at 244 K.

B. High-Temperature Adsorption. The second set of experiments is taken from the series of adsorption isotherms first reported in ref 2 between 180 and 200 K. In these experiments, pHCl and pH₂O were detectable throughout the experiment, and the coverage of the surface by HCl as a function of pHCl at constant temperature was measured, followed in some cases by heating of the sample. The experiments were carried out on ice *I_h* samples of 8 m²/g ($\pm 20\%$) total area. The HCl was introduced without carrier gas at constant rates of approximately 10⁻⁸ mol/s. The measured isotherms were demonstrated to be invariant to the total ice surface area and representative of an equilibrium state with the gas phase at these rates of introduction.² The ice pressure, pH₂O, was constant at that over pure ice *I_h* during adsorption but varied as a function of pHCl subsequent to the nucleation of a bulk phase, as will be discussed below. Three representative isotherms are shown in Figure 2, plotted as pHCl as a function of pH₂O at 180, 190, and 200 K. The data are superimposed on the HCl/H₂O bulk binary phase diagram, calculated using the AIM model¹⁷ from Carslaw et al.¹⁸ The solid black lines are the bulk phase boundaries separating the trihydrate, hexahydrate, ice, and liquid regions. The solid gray lines are calculations of pHCl and pH₂O over equilibrium binary solutions. The lines are isotherms of constant temperature (labeled); therefore, concentration is changing implicitly along these lines. The solid lines are calculations at temperatures within the parametrized range of the AIM model. The dashed gray lines are also solution isotherms, now calculated by extrapolating the results of the AIM model to temperatures below the parametrized range. This was accomplished by plotting pHCl and pH₂O for constant solution concentrations as a function of temperature. This temperature dependence was then fit to a Clausius–Claypyron equation for each pressure, and this equation was used to calculate the low-temperature pressure for that solution concentration. Repeated calculation at different concentrations

generated the isotherms. We note that there is essentially no data to support the AIM model calculations at temperatures below 180 K, which is the low-temperature end of the range of parametrization of the model. The open points are determinations of hydrate and bulk liquid nucleation discussed below.

Discussion

A. Low-Temperature Adsorption and Heating. We interpret the SHG intensity as a function of temperature in this experiment in a manner similar to that in ref 2. The low but detectable intensity obtained from the ice surface at the beginning of the experiment is consistent with levels measured in numerous experiments in our laboratory from the surface of annealed, porous ice *I_h* at low temperature. At 110 K, the SHG intensity falls below detection limits. A similar loss of intensity has been measured reliably at the bulk melting point of hydrate phases and of ice with submonolayer amounts of HCl adsorbed.² This loss in SHG signal at 110 K is therefore attributed to the nucleation of a surface metastable solution, consistent with the expected phase of the system at HCl concentrations above a monolayer and before the hydrate nucleation boundary. The rise in SHG signal at 156 K and loss again at 202 K is similarly attributed to the nucleation and subsequent melting of the bulk hexahydrate phase, again consistent with past observations.² The rise in pHCl at 110 K is attributed to the partial pressure expected over the metastable solution, as will be shown below. The decrease in pHCl between 152 and 202 K is due to the formation and growth of the hexahydrate and, therefore, does not represent an equilibrium vapor pressure. After 202 K, however, pHCl is again the equilibrium partial pressure above the melted solution, as will be shown below.

We have replotted the data of Figure 1 in Figure 3, where we plot ln(pHCl) and SHG intensity now as a function of the inverse temperature. Using the SHG intensity as an indication of the presence of the bulk hexahydrate phase, Figure 3 has been divided into three regions as a function of temperature and labeled as ‘metastable solution’, denoting a phase of HCl on the ice before bulk hydrate nucleation; ‘hexahydrate’, indicating the formation of the equilibrium bulk phase at the surface; and ‘liquid’, indicating the melting of the hydrate phase to a solution. The linear relationship of ln(*P*) to 1/*T* in the metastable solution and liquid ranges indicate partial pressures

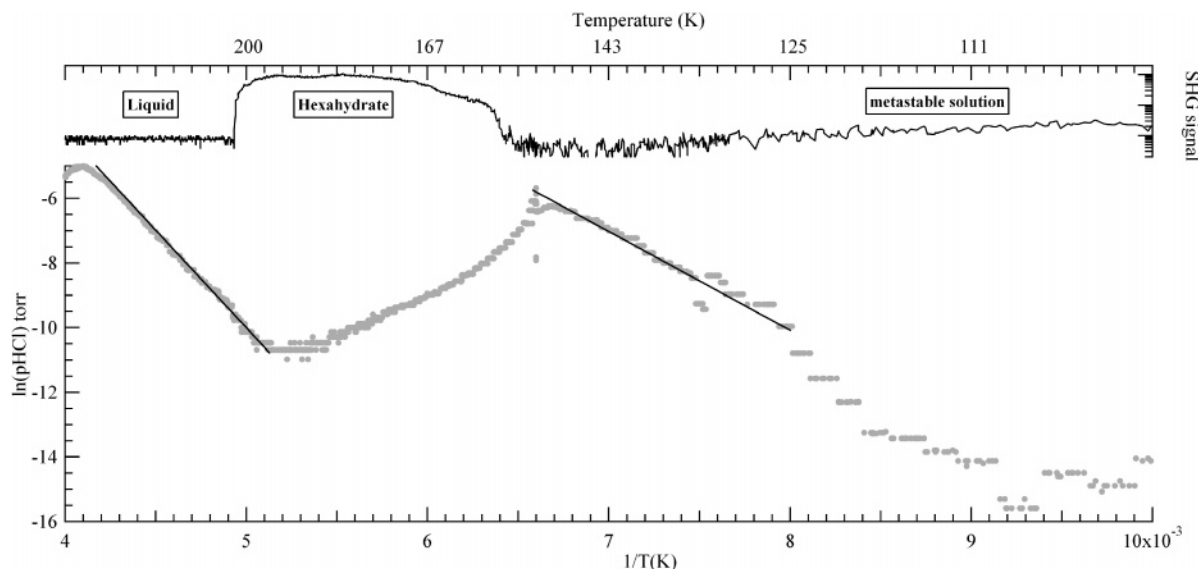


Figure 3. Measured SHG intensity (solid curve) and HCl pressure, $\ln(\text{pHCl})$, (gray points) from Figure 1 replotted as a function of the inverse temperature. The three phases of HCl and H_2O exhibited in this experiment are labeled in the temperature range where they were observed. The bold lines through the gray data are calculations of pHCl as a function of temperature over an 8.67 M (200–230 K) and 20.33 M (125–150 K) HCl solution. The pressure was calculated from Carslaw et al.¹⁸ using the AIM model.¹⁷

controlled by single Clausius–Clapyron enthalpies and that, therefore, the HCl/ H_2O system is in equilibrium (albeit metastable in the former phase) in these ranges.

The solid black lines are calculations of pHCl and pH_2O over two solutions of constant concentration, calculated as a function of the temperature again from the AIM model (extrapolated in the low-temperature case outside of the parametrized temperature range). The calculated concentration of the low-temperature metastable solution is 20.33 M HCl, or 2.73 mol H_2O per mole of HCl. The calculated pHCl is shown over a temperature range beginning at about 125 K. pHCl between 110 and 125 K does not agree with this calculated concentration, indicating that over this range the system is undergoing a kinetically dominated period where the solution is approaching the metastable equilibrium concentration exhibited by the phase between 125 and 150 K. It is important to note that nucleation of the metastable solution occurs deep within the region of the bulk binary phase diagram where the trihydrate is the true equilibrium bulk phase; reflected in the near 3 to 1 stoichiometry of the metastable solution. The calculated concentration of the high-temperature bulk solution is 8.81 M HCl, or 6.3 mol H_2O per mole of HCl. This concentration is also consistent with the bulk phase diagram, and reflects the 6 to 1 stoichiometry of the melted hexahydrate phase.

This experiment thus exhibits a very informative trajectory on the HCl/ H_2O phase diagram. Although there is not sufficient information to comment on the original surface state of the adsorbed HCl on ice below 110 K, nucleation of a metastable surface solution is inferred from SHG intensity. This is consistent with the observations of nucleation at higher temperatures subsequent to monolayer adsorption. The resulting solution reflects the equilibrium concentration expected of a bulk binary HCl/ H_2O solution under these conditions. The nucleation of the bulk hexahydrate is observed at measured temperature and pHCl of 150 K and 2 mTorr. Subsequent to nucleation, the available HCl is incorporated into the ice at the hexahydrate stoichiometry, presumably liberating the necessary H_2O from the ice surface. Melting the hexahydrate phase yields an equilibrium bulk solution whose concentration is again consistent with the bulk phase diagram.

B. Hexahydrate Nucleation Boundary. The compilation of data from this and other laboratories regarding the nucleation of the bulk hexahydrate from the metastable solution is shown in Figure 2. The open square in Figure 2 is the point at which the hydrate was observed to nucleate in the experiment of Figure 1. The point is plotted as the measured pHCl versus calculated pH_2O . pH_2O was calculated from the extrapolated 150 K solution isotherm. The inverted open triangle data point is determined from a set of adsorption experiments reported by Banham et al.⁵ The data were reported as the pHCl necessary to nucleate the crystalline hexahydrate at 165 K. For comparison, the measured pHCl versus pH_2O calculated from the extrapolated 165 K solution isotherm is shown. The open triangle data point is determined from a set of uptake experiments reported by Abbatt et al.¹⁹ In those experiments, it was noted that hexahydrate nucleation was only observed subsequent to cooling ice samples dosed with HCl to temperatures below 170 K and then warming them. In order to determine a nucleation boundary from these results, the average of the reported pHCl in those experiments versus pH_2O calculated from the extrapolated 170 K solution isotherm is shown. The error bar in pHCl reflects the full pressure range. The open circle data points plotted along the 180, 190, and 200 K solution isotherms were obtained from the adsorption experiments described in ref 2. The open circles at 180 and 190 K denote the measured pHCl and pH_2O at the point where hexahydrate nucleation was observed by simultaneous SHG measurement. The open circle along the 200 K solution isotherm was determined as the point at which nucleation of the bulk liquid was observed, again by SHG.

Beginning with the first modern measurements by Vuillard,²⁰ the difficulties of nucleating the hexahydrate phase have often been commented upon. In early work related to the stratosphere, Hanson and Mauersberger²¹ were unable to nucleate the hexahydrate from the vapor. Quick consensus was reached that nucleation was achieved only via the supercooled melt^{19,22,23} or amorphous phase.⁵ The observations of nucleation reported here are consistent with this observation, as nucleation has only been observed in this laboratory from the metastable solution nucleated subsequent to monolayer uptake of HCl. Furthermore, the dashed line of Figure 2, which links the various measure-

TABLE 1: Solution Free Energy, G_{sol} , Calculated Using Eq 1

T (K)	pHCl (Torr)	pH ₂ O (Torr)	G_{sol} (kJ/mol)
150	2.00×10^{-3}	1.50×10^{-9}	49.64
165	4.56×10^{-5}	8.00×10^{-7}	51.17
170	5.50×10^{-5}	2.00×10^{-6}	51.16
180	2.20×10^{-5}	4.50×10^{-5}	50.88
190	1.50×10^{-5}	2.00×10^{-4}	51.96
200	8.00×10^{-6}	1.60×10^{-3}	52.28

ments and calculations of nucleation pressures as a function of temperature, represents a locus of points defining a state of constant liquid free energy. While the nucleation mechanism remains unclear, this locus of points provides some clue as to the origin. We define the ideal solution free energy as

$$G_{\text{sol}} = RT \ln \left(\frac{(\text{pHCl})(\text{pH}_2\text{O})}{p_o^2} \right) \quad (1)$$

where T is the temperature, R the ideal gas constant, and p_o is a standard state pressure, 760 Torr. The pHCl, pH₂O, and T for each nucleation point in Figure 2 and the resulting G_{sol} are shown in Table 1. The calculated free energy is 51.2 ± 0.9 kJ/mol. It is not clear at this time how this absolute energy might combine with the free energy of the equilibrium hexahydrate phase to define a free energy difference or define a solid nucleation free energy. Work continues to address these issues.

C. Metastable Solution Boundary. The nucleation of the metastable melt subsequent to monolayer coverage of ice by HCl was first noted in Henson et al.² It was not noted in that work, however, that an extrapolation of the bulk ice/liquid coexistence line on the binary bulk phase diagram was likely the thermodynamic boundary between the submonolayer uptake of HCl and the formation of the metastable solution. This coexistence line is, however, the thermodynamic boundary separating submonolayer adsorption of HCl by ice and the nucleation of the metastable binary bulk solution, as will be shown below. Furthermore, the observation by SHG of the nucleation of the melt at 110 K extends the validity of this extrapolated boundary to 110 K. The submonolayer adsorption of HCl according to ref 2 at pHCl below this boundary is therefore also inferred to 110 K. Earlier qualitative indications of this boundary between regions of relatively low and high HCl uptake were provided by Abbatt et al. in early HCl uptake experiments related to stratospheric heterogeneous chemistry.¹⁹

The model of submonolayer adsorption of HCl on ice determined in ref 2 is consistent with this boundary. The calculated adsorption isotherms for HCl on ice at temperatures from 150 to 190 K are shown in Figure 4. The isotherms are calculated using, from ref 2

$$P = (2\pi mkT)^{3/2} \frac{kT}{h^3} \left(\frac{f\theta}{1-f\theta} \right)^f q_{\text{U}}^{-3v} q_{\text{A}}^{-3\alpha} \exp(-(\alpha\Delta E_{\text{A}} + v\Delta E_{\text{U}} + f^2\theta\epsilon)/RT) \quad (2)$$

where P (Torr) and m (kg) are the HCl pressure and molecular mass, k and h are Boltzman's and Plank's constants, T is the absolute temperature, and θ the coverage calculated from the total number of HCl molecules adsorbed. The q_i refer to the translational components of the two molecular partition functions describing the two adsorption states in the system: the unassociated state U, where dissociated H⁺ and Cl⁻ ion adsorb into two distinct sites, and the associated state A, where the ions occupy a single site. The adsorption energies into the U or A

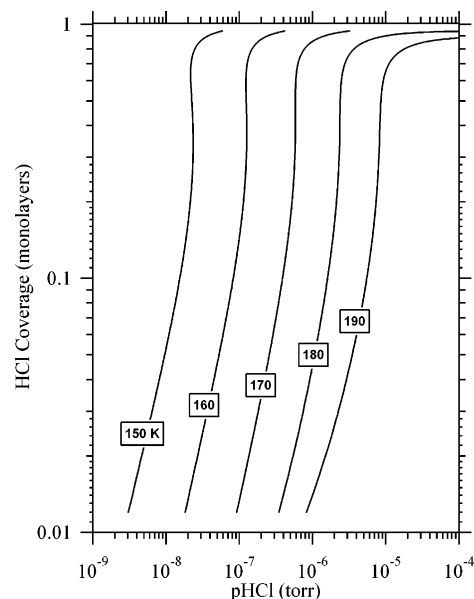


Figure 4. Calculated adsorption isotherms for HCl on ice plotted as the coverage of the surface as a function of HCl pressure from 150 to 190 K. The calculations were performed using eqs 2–5 with the parametrization listed in Table 2.

TABLE 2: Parametrization of Eq 2

	ΔE_{U} (kJ/mol)	ΔE_{A} (kJ/mol K)	ϵ (kJ/mol)	ϕ_{A} (K)	ϕ_{U} (K)
ice	0.2	30.8	5.4	3.05	2.11

ionic states are given by ΔE_{U} and ΔE_{A} , respectively, and ϵ denotes a lateral interaction energy between occupied sites. The q_i are given by

$$q_i = \exp\left(-\frac{\phi_i}{2T}\right) \left(1 - \exp\left(-\frac{\phi_i}{T}\right)\right) \quad (3)$$

where i is either U or A, using either ϕ_{U} or ϕ_{A} as the vibrational temperature. The exponents f , α and v are functions of coverage and the relative surface concentrations of the two states. They are given by $f = 1 + \chi$, $\alpha = 1 - \chi$, and $v = \chi$, where

$$\chi = \frac{\sqrt{(K + 2\theta)^2 - 4\theta - K}}{2\theta} \quad (4)$$

and the relative surface concentrations are controlled by a surface equilibrium constant K which is given by

$$K = \frac{q_{\text{U}}^2}{q_{\text{A}}} = \frac{\left(\exp\left(-\frac{\phi_{\text{U}}}{2T}\right) \left(1 - \exp\left(-\frac{\phi_{\text{U}}}{T}\right)\right)\right)^6}{\left(\exp\left(-\frac{\phi_{\text{A}}}{2T}\right) \left(1 - \exp\left(-\frac{\phi_{\text{A}}}{T}\right)\right)\right)^3} \exp(4\Delta E_{\text{U}} - \Delta E_{\text{A}}) \quad (5)$$

The constants for HCl adsorption on ice used in eqs 2–5 are given in Table 2.

The coverage of the ice surface is calculated as a function of pressure in Figure 4. The total coverage is shown, without any reference to the relative coverage by the associated or unassociated states, although the effects of unassociated state coverage are apparent in the slope at low coverage of the isotherms at 180 and 190 K. The HCl coverage at a monolayer was

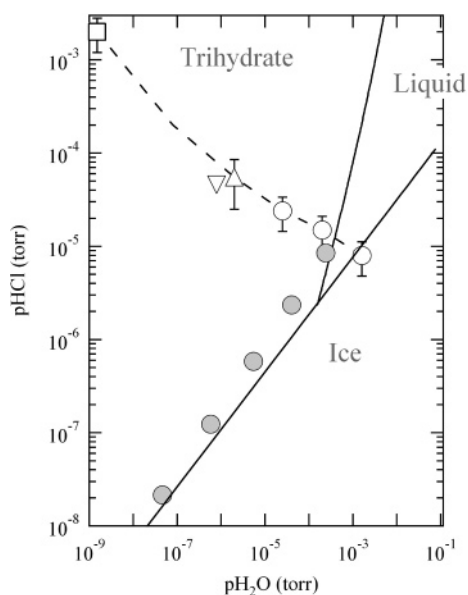


Figure 5. Bulk phase nucleation boundaries superimposed on the HCl/H₂O bulk phase diagram. The black lines denote the coexistence boundaries between bulk phases, as labeled. The bulk trihydrate/liquid coexistence boundary is calculated from Carslaw et al.¹⁸ using the AIM model.¹⁷ The ice/liquid coexistence boundary is an extrapolation outside the range of parametrization of the AIM model. The gray data points denote the boundary for the nucleation of the metastable solution subsequent to monolayer adsorption. They are the calculated HCl pressures at monolayer adsorption taken from the isotherms of Figure 4, plotted as a function of the ice vapor pressure at that temperature. The open points and the black dashed line denote the hexahydrate nucleation boundary, as in Figure 2.

determined to be 2.3×10^{14} molecules/cm².² As discussed previously,² the isotherms exhibit non-Langmuir behavior, with uptake just prior to monolayer coverage extremely sensitive to pressure. The asymptotic rise in pressure at monolayer uptake is observed in experiments but is not due to adsorption. As soon as pressure begins to rise in the experiment, the metastable solution is nucleated and the isotherm is no longer valid, giving way instead to solution concentrations and rising partial pressures predicted from the bulk binary phase diagram.

We define the relatively constant pHCl just prior to nucleation of the metastable solution to be the nucleation boundary, and we plot this pHCl as a function of the ice vapor pressure for each of the isotherms of Figure 4 as the gray circles in Figure 5. Also plotted in Figure 5 are the points and dashed black line denoting the solid hydrate phase boundary. The two solid black lines are the trihydrate/liquid phase boundary, calculated as before¹⁸ and an extrapolation of the ice/liquid phase boundary calculated using the AIM model.¹⁷ The calculation is a fit to the ice/liquid boundary, again extrapolated outside the range of parametrization in the AIM model. The pertinent comparison is the gray points and the ice/liquid phase boundary. Although the points predicted by the adsorption isotherm, eq 2, follow a somewhat steeper slope than ice/liquid coexistence, the comparison is favorable over this temperature range, spanning 150–190 K. It is important to stress that the adsorption isotherm was determined only from the observed adsorption behavior of HCl over the range 180–200 K and not fit with any preconceived notions regarding the metastable solution nucleation or the proximity to the ice/liquid coexistence line. As such, the agreement of the nucleation boundary as calculated from the adsorption isotherm with the ice/liquid coexistence line serves as a prediction of this surface nucleation boundary. Having identified this thermodynamic boundary between adsorption and

nucleation of the metastable bulk solution, we could return to the adsorption data and refit the parametrization to better reflect the boundary, but the improvement in fit to both the coexistence line and the observed nucleation points would be minor.

D. Reversibility. It was not possible to determine thermodynamic reversibility in this system as a function of concentration. While it was possible to equilibrate the system sufficiently rapidly during introduction of HCl at low rates,² attempts to reduce the HCl content of the system by application of vacuum led to perturbations in surface temperature as well. In addition, the rate of HCl loss from the ice surface is controlled by sublimation or vaporization rates which were observed to be too slow to allow for the removal of appreciable amounts of HCl on the time scale of the experiment. We did, however, observe the SHG signal from the equilibrium bulk hexahydrate to be persistent upon cooling of the sample, indicating the irreversible formation of the equilibrium bulk phase, as expected.

Conclusions

These new measurements and modeling provide a complete description of the interaction of HCl with ice at these temperatures and pressures. From the adsorption isotherm described by Henson et al.,² the initial low-pressure interaction of HCl with ice is through complete dissociation during adsorption onto the ice surface to occupy either of two states. In one state, the unassociated state, the ions are separate and occupy two distinct sites, in a manner analogous to a two-dimensional lattice gas phase. In the other, associated state, the ions both occupy one site, in a manner analogous to descriptions of contact ion pairs in molecular dynamics calculations of the interaction of HCl with ice.²⁴ The relative concentrations of the two states are controlled by a temperature-dependent equilibrium constant, with the unassociated state favored at high temperature and low coverage and the associated state favored at low temperature and high coverage. The state is strictly two-dimensional until saturation at monolayer coverage drives pHCl asymptotically higher, quickly resulting in the nucleation of a metastable bulk solution. As shown here, this occurs at the ice/liquid coexistence line on the binary bulk phase diagram. Subsequent heating or introduction of more HCl drives pHCl higher until a second nucleation boundary is encountered where the final equilibrium solid hexahydrate phase is nucleated. This boundary is defined as a locus of points in *T* and pHCl and pH₂O that constitute a constant solution free energy defined by eq 1.

The role of the underlying ice phase in all the experiments reported here and in ref 2 has been observed to be either an inert surface substrate or a reservoir of H₂O necessary to form the observed bulk phases. As an inert surface, pH₂O is observed to be independent of pHCl and constant at the ice vapor pressure during submonolayer adsorption. Subsequent to the nucleation of bulk phases pH₂O varies as predicted by the bulk phase diagram for solutions of (metastable) equilibrium concentration or over the hexahydrate. Also subsequent to nucleation, the ice surface presumably contributes the H₂O necessary to combine with HCl to form these solutions. In all experiments reported here and in ref 2, the amount of HCl introduced was insufficient to completely convert all of the ice into any one bulk phase, and all adsorbed, metastable, and equilibrium solution and hexahydrate phases were observed to exist on top of the remains of the initial ice lattice.

Finally, with the observation of metastable solution formation at 110 K reported here, as well as bulk melting in ref 2, we determine the applicability of this model of HCl interaction with ice to be valid over a temperature range spanning 110–200 K.

Acknowledgment. B.F.H. acknowledges helpful discussions with Simon Clegg and Anthony Wexler regarding the use of the AIM model. This work was funded by the Laboratory Directed Research and Development Projects entitled "Classic Kinetic Mechanisms Describing Heterogeneous Ozone Depletion (97023ER)" and "Resolving the Aerosol-Climate-Water Puzzle (20050014DR)" administered by Los Alamos National Laboratory for the Department of Energy.

References and Notes

- (1) Solomon, S. *Rev. Geophys.* **1999**, *37*, 275.
- (2) Henson, B. F.; Wilson, K. R.; Robinson, J. M.; Noble, C. A.; Casson, J. L.; Worsnop, D. R. *J. Chem. Phys.* **2004**, *121*, 8486.
- (3) Buch, V.; Sadlej, J.; Aytemiz-Uras, N.; Devlin, J. P. *J. Phys. Chem. A* **2002**, *106*, 9374.
- (4) Uras, N.; Rahman, M.; Devlin, J. P. *J. Phys. Chem. B* **1998**, *102*, 9375.
- (5) Banham, S. F.; Sodeau, J. R.; Horn, A. B.; McCoustra, M. R. S.; Chesters, M. A. *J. Vac. Sci. Technol., A* **1996**, *14*, 1620.
- (6) Delzeit, L.; Powell, K.; Uras, N.; Devlin, J. P. *J. Phys. Chem. B* **1997**, *101*, 2327.
- (7) Lu, Q. B.; Sanche, L. *J. Chem. Phys.* **2001**, *115*, 5711.
- (8) Kang, H.; Shin, T. H.; Park, S. C.; Kim, I. K.; Han, S. J. *J. Am. Chem. Soc.* **2000**, *122*, 9842.
- (9) Park, S. C.; Kang, H. *J. Phys. Chem. B* **2005**, *109*, 5124.
- (10) Donsig, H. A.; Vickerman, J. C. *J. Chem. Soc. Faraday Trans.* **1997**, *93*, 2755.
- (11) Bournel, F.; Mangeney, C.; Tronc, M.; Laffon, C.; Parent, P. *Surf. Sci.* **2003**, *528*, 1.
- (12) Herring, J.; Aleksandrov, A.; Orlando, T. M. *Phys. Rev. Lett.* **2004**, *92*, 187602.
- (13) Devlin, J. P.; Gulluru, D. B.; Buch, V. *J. Phys. Chem. B* **2005**, *109*, 3392.
- (14) Uras-Aytemiz, N.; Joyce, C.; Devlin, J. P. *J. Phys. Chem. A* **2001**, *105*, 10497.
- (15) Rudzinski, W.; Everett, D. H. *Adsorption of Gases on Heterogeneous Surfaces*; Academic Press, 1992.
- (16) Wagner, W.; Saul, A.; Pruss, A. *J. Phys. Chem. Ref. Data* **1994**, *23*, 515.
- (17) Clegg, S. L.; Brimblecombe, P. On-Line Aerosol Inorganics Model. <http://www.hpc1.uea.ac.uk/~e770/aim.html>.
- (18) Carslaw, K. S.; Clegg, S. L.; Brimblecombe, P. *J. Phys. Chem.* **1995**, *99*, 11557.
- (19) Abbatt, J. P. D.; Beyer, K. D.; Fucaloro, A. F.; McMahon, J. R.; Wooldridge, P. J.; Zhang, R.; Molina, M. J. *J. Geophys. Res. Atmos.* **1992**, *97*, 15819.
- (20) Vuillard, G. C. *Ann. Chem. Paris* **1957**, *13*, 233.
- (21) Hanson, D. R.; Mauersberger, K. *J. Phys. Chem.* **1990**, *94*, 4700.
- (22) Koehler, B. G.; McNeill, L. S.; Middlebrook, A. M.; Tolbert, M. A. *J. Geophys. Res. Atmos.* **1993**, *98*, 10563.
- (23) Wooldridge, P. J.; Zhang, R. Y.; Molina, M. J. *J. Geophys. Res. Atmos.* **1995**, *100*, 1389.
- (24) Gertner, B. J.; Hynes, J. T. *Faraday Discuss.* **1998**, *110*, 301.